

# Wind and Irradiance Observations of Jupiter's Aurora using JOVE

Jupiter Observations of Velocity and Emissions (JOVE)

Andrew Bell, W.E.Ward, J.C. McConnell & B. Solheim

ESTEC Jan 19<sup>th</sup> 2010



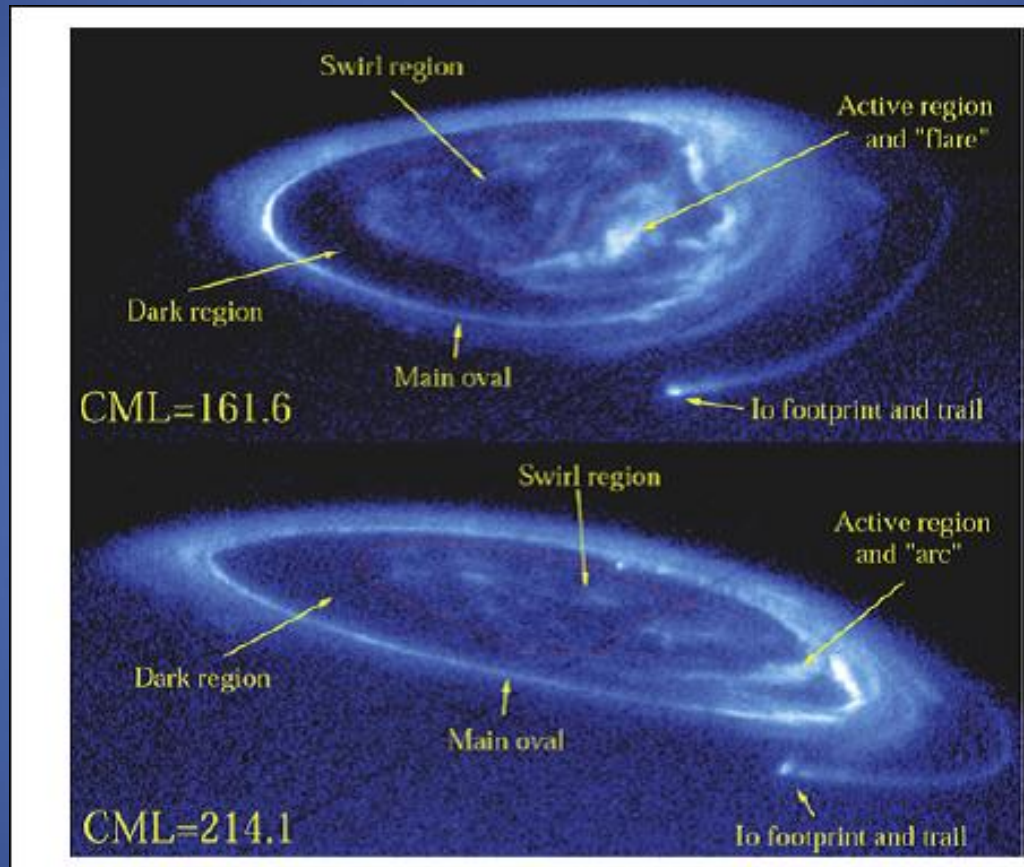
# Science Overview

The temperature of the thermosphere of Jupiter is observed to be 1000 K which cannot be explained by the heating by solar EUV provides no more than a temperature of  $\sim 150$  K. Upward propagating gravity waves which then deposit energy and momentum or particle precipitation from the magnetosphere have both been suggested as energy sources. Auroral energy deposition could also provide a major energy source if the thermospheric circulation could re-distribute this energy – clearly wind measurements are needed.

The ionosphere with a solar EUV ionization source would provide a peak electron density of  $\sim 1\text{E}6$  e/cm<sup>3</sup> while measured peak densities are much more and are much higher than calculated by simple or even 3D models. There is a suggestion that H<sub>2</sub> may have very high vibrational temperature  $\sim 2000$ -4000 K which is likely to affect ion chemistry. In addition the ion peak that occurs at high latitudes can (theoretically) only be sustained by vertical winds.

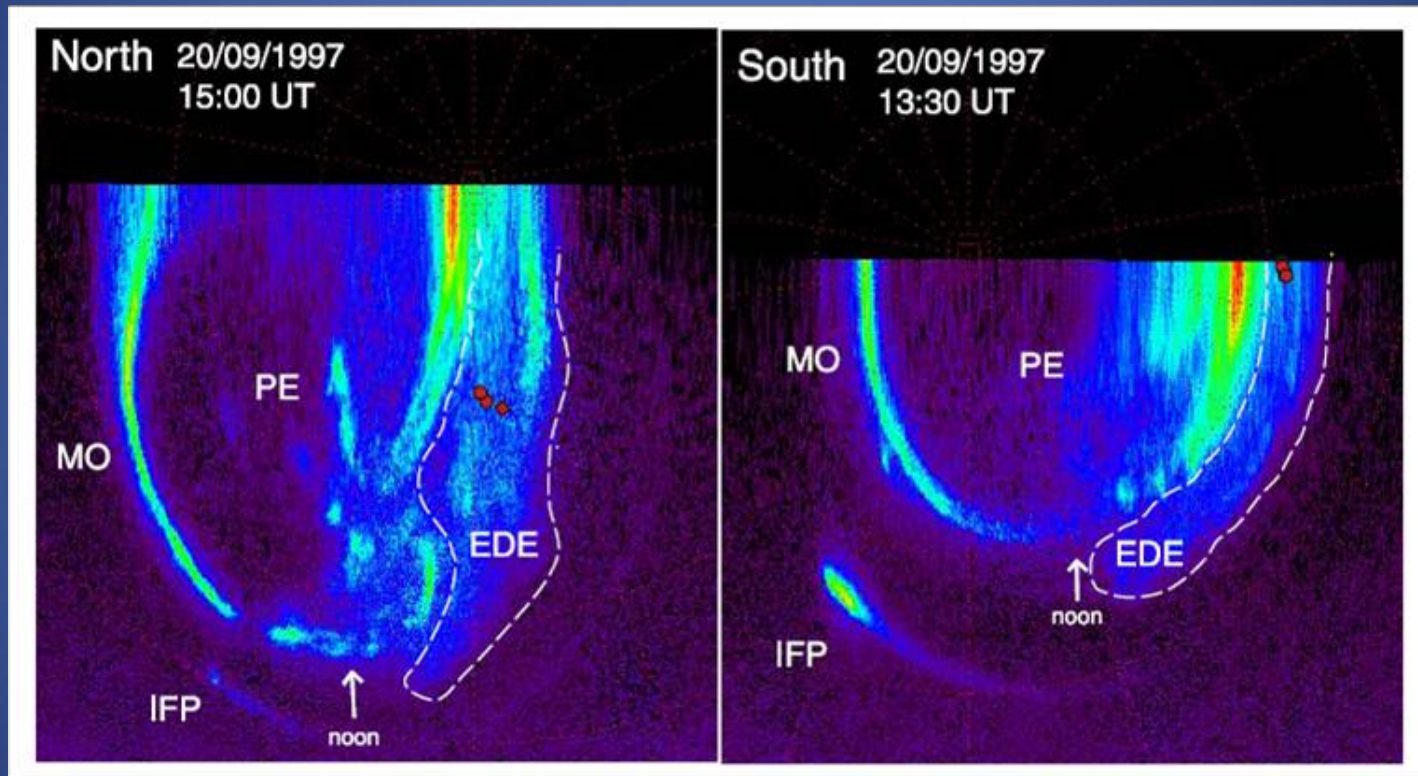
A high resolution interferometer, JOVE, is proposed to measure wind and emission rate (and possibly temperature) using H<sub>3</sub><sup>+</sup> and H<sub>2</sub> lines near 2 microns. The emissions chosen would provide information on ion or neutral winds as well as the morphology of the constituents which play important roles in the energy budget of this region of the atmosphere. They would provide evidence of propagating gravity waves and other energy sources.

# UV images of Auroral Oval



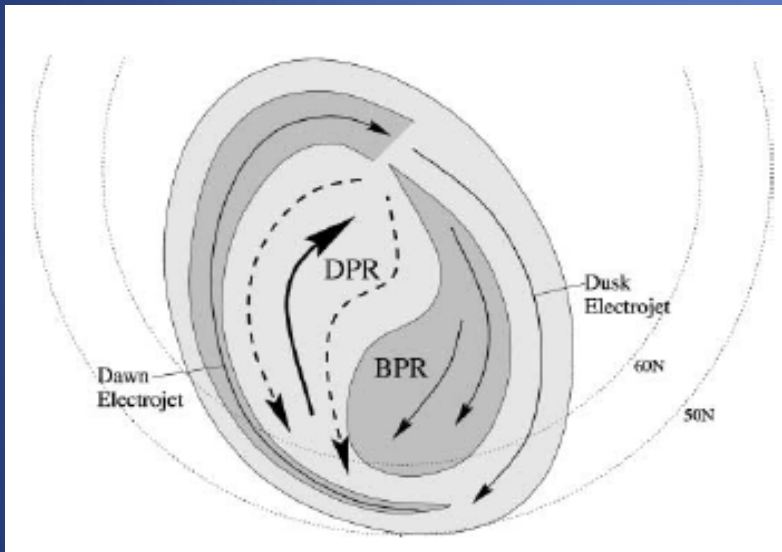
Grodent et al., JGR, 2003

# Morphology of Auroral Emissions

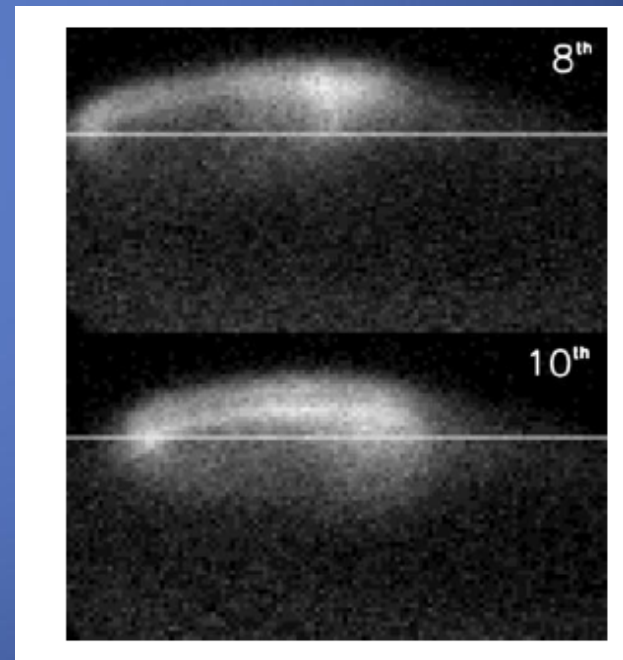
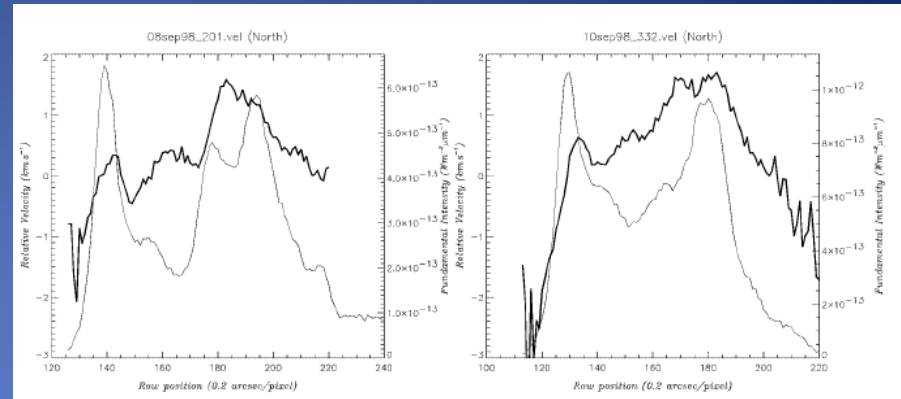


Radioti et al., GRL, 2009: HST FUV images

# Ion Winds Earth Based

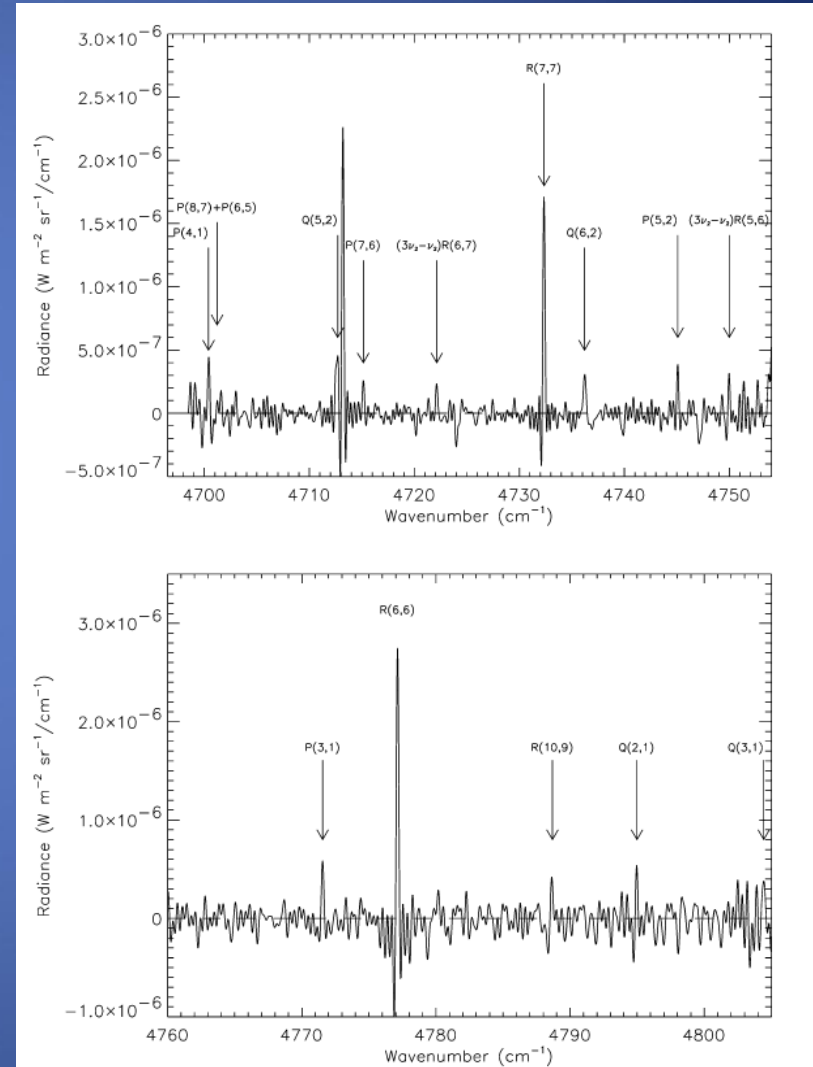


Stallard et al., (Icarus, 2001), published winds measured from the Earth using emissions from the Q(1,0-) line in the fundamental  $v_2$  ( $v_2 = 1 \rightarrow 0$ ) vibrational band of the  $H_3^+$  molecular ion, which occurs at  $3.9530 \mu\text{m}$ .



# Auroral Emissions near 2 microns

- The preliminary emissions targeted for JOVE are the  $\text{H}_2 \text{S}_1(1)$  line at  $4713 \text{ cm}^{-1}$  and the neighbouring  $\text{H}_3^+$  lines (Q(5,2) and P(7,6) and the strong R(7,7) line.
- These would provide information on both the ion and neutral velocities and the emission rates (and possible temperature) of the two target species.
- Observations are ideally taken in the limb but information from other observations geometries are of interest.



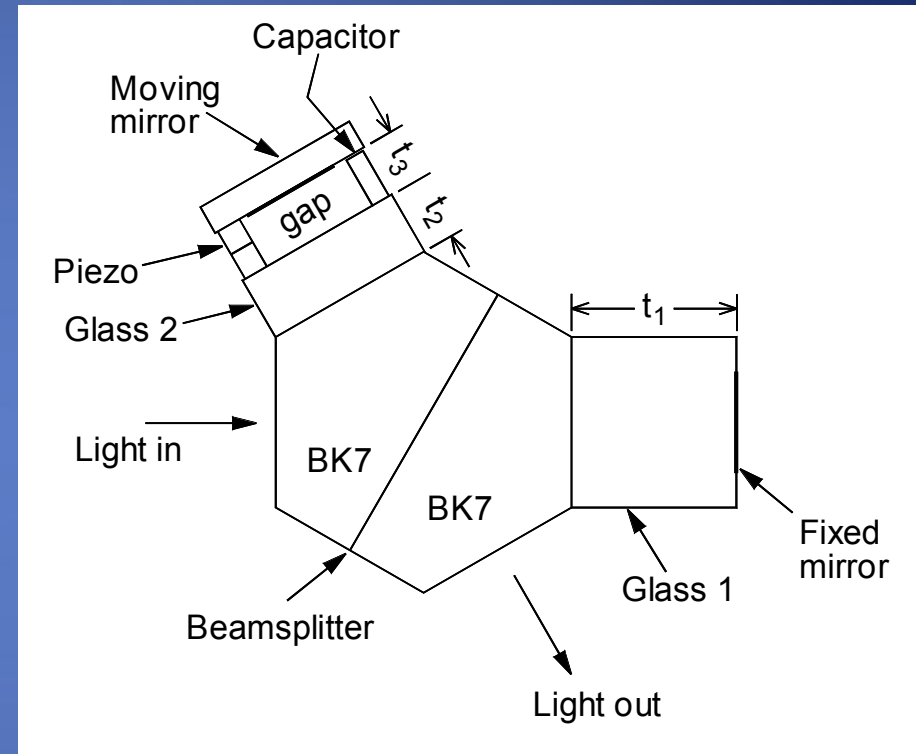
Reynaud et al., Icarus, 2004

# Instrument Possibilities

- Three potential instrument possibilities exist:
  - Doppler imaging through a field-widened Michelson interferometer.
  - A field-widened polarization interferometer
  - Spatial Hetrodyne Spectroscopy

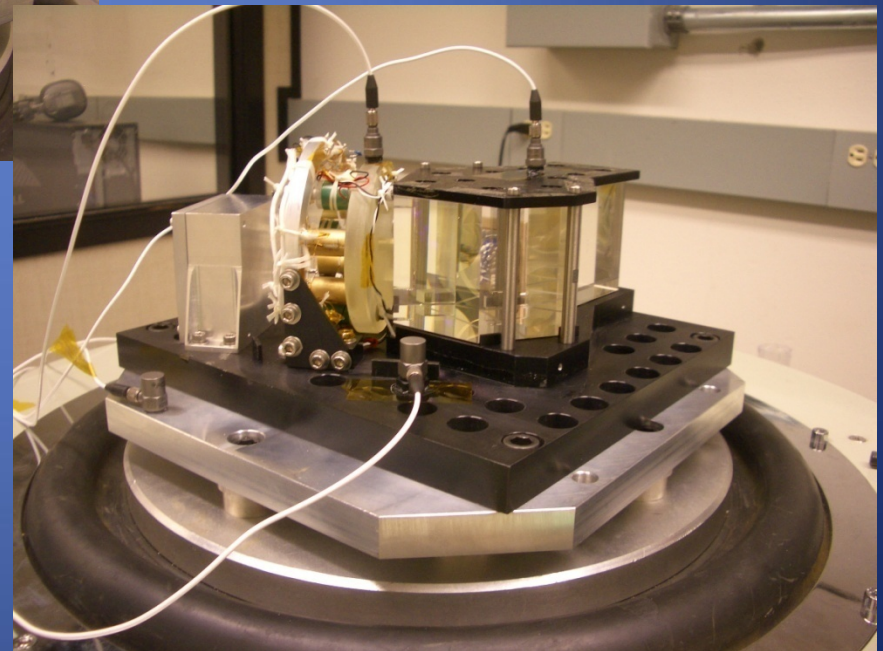
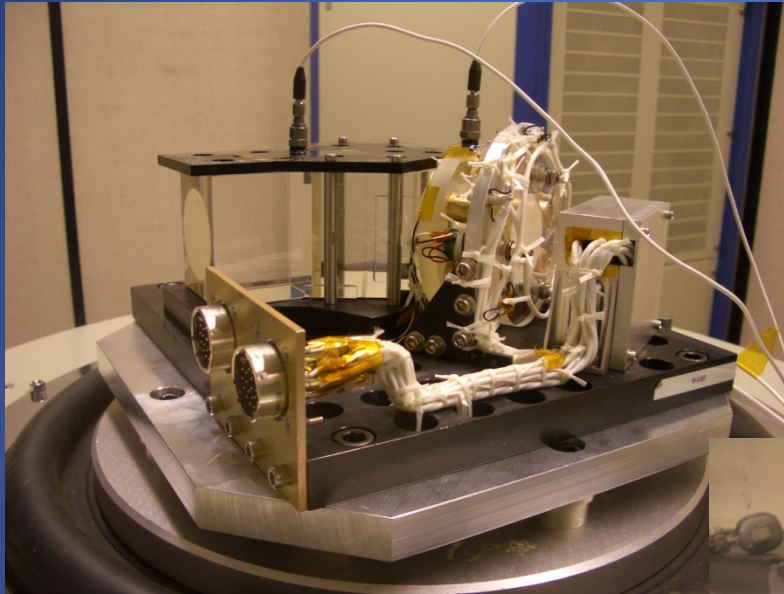
# Example Instrumentation Design: Doppler Imaging Interferometer

Glasses	Arm lengths (cm)
N-LAK12	$t_1 = 5.9616$
SF11	$t_2 = -2.2513$
gap	$t_3 = -2.2787$



- $\Delta = 7.4$  cm – actual path difference TBD
- Field widening allows a large angular field and hence large throughput through the instrument.
- Integrations time depend on the emission intensity, spatial and velocity resolution appropriate for science objectives.

# Field Widened Michelson under TRL6 Vibration test



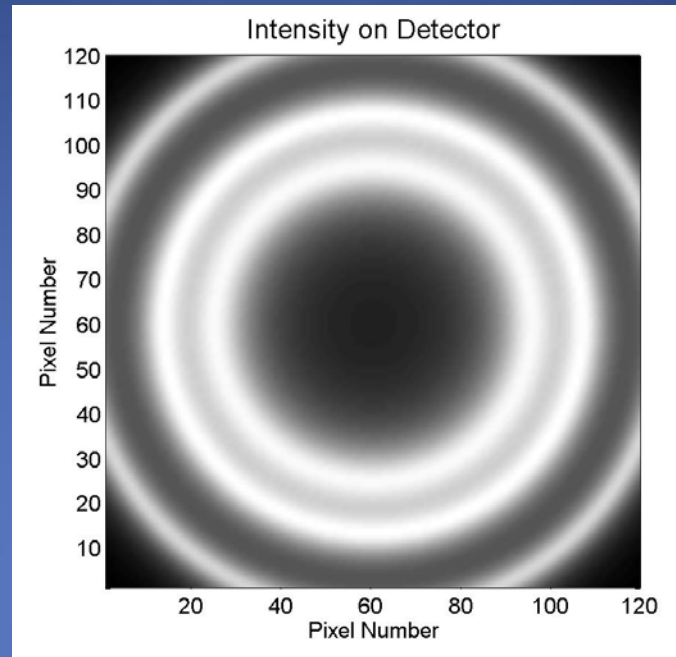
Other Heritage;

Etalon, angstrom positioning, JWST  
30K, F2T2 - Gemini

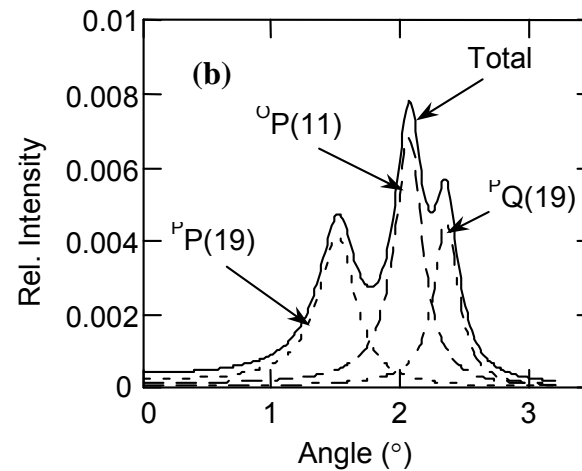
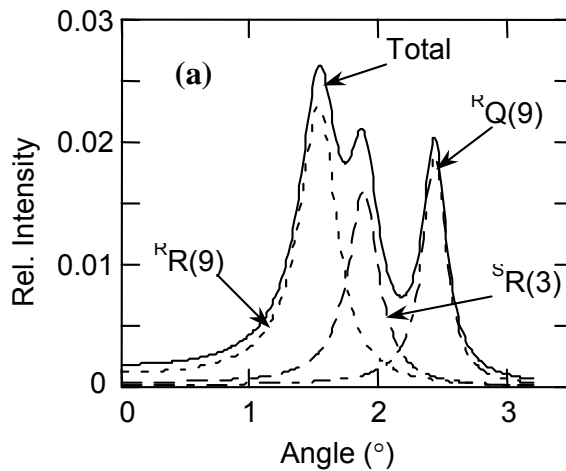
Optical field units for Earth  
Measosphere airglow measurements

SWIFT @10 $\mu$ m, WINDII on UARS

# Spatial/Spectral Application



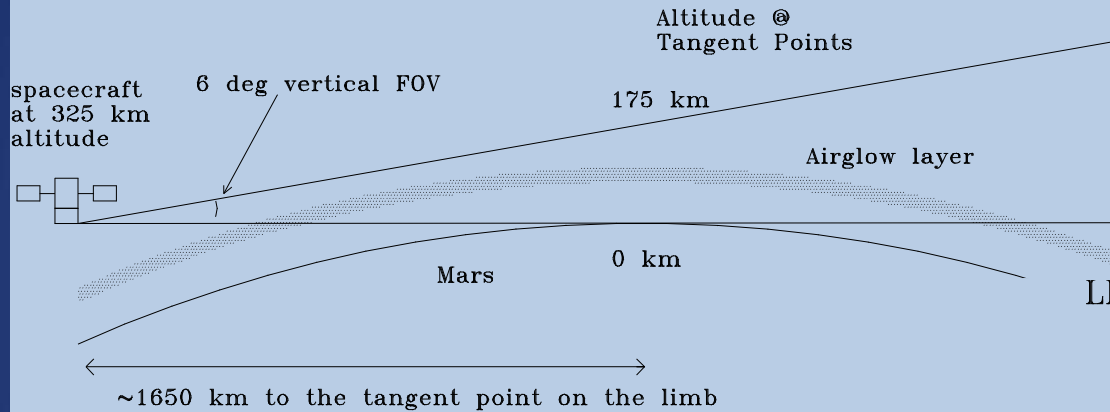
Example of spatial spectral separation of emission lines from the O<sub>2</sub> IR Atmospheric band using an etalon.



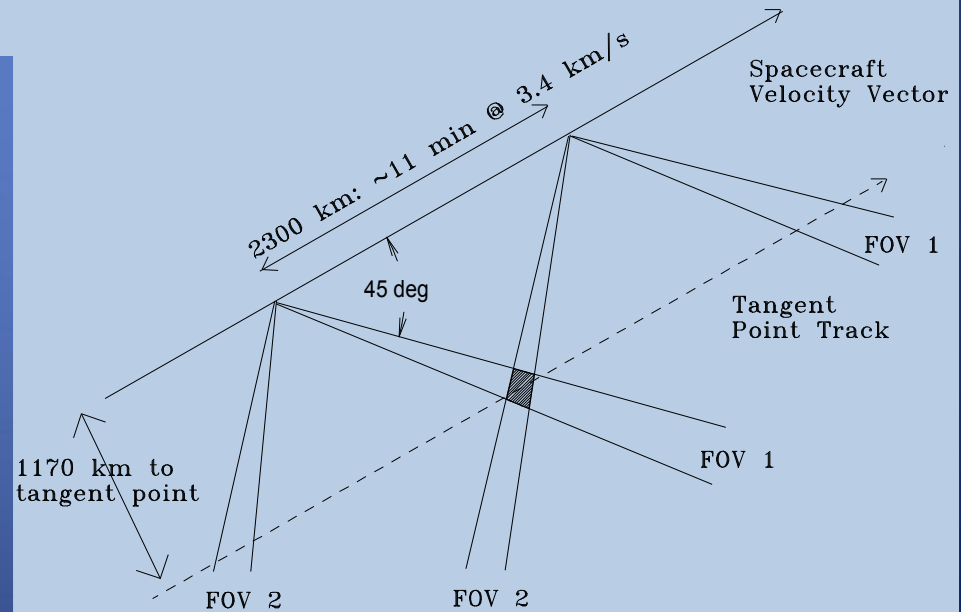
Relative intensity as a function of incident angle seen through the etalons for the (a) strong and (b) weak O<sub>2</sub> lines

# Mars – Geometry of Observations

LIMB IMAGING GEOMETRY  
SIDE VIEW



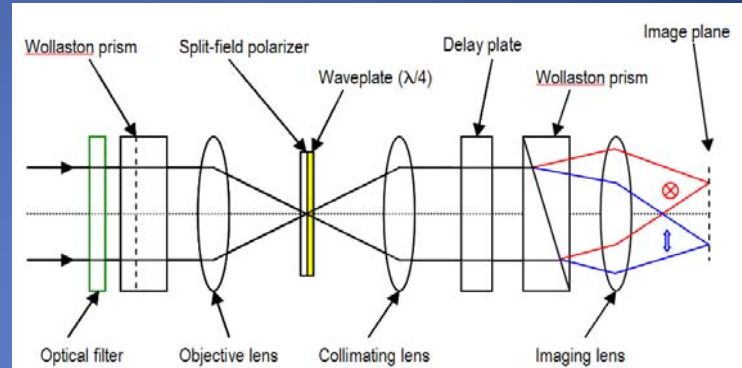
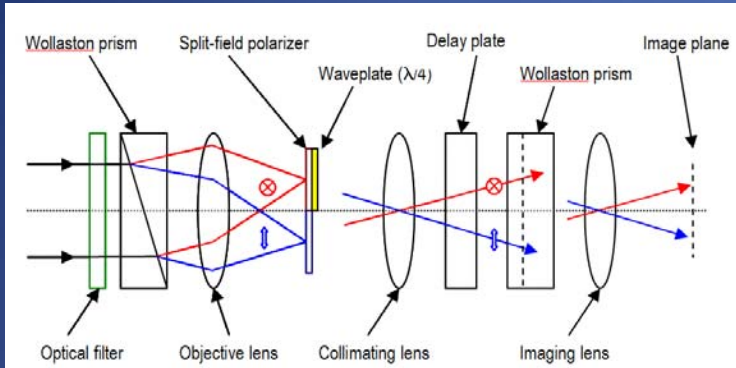
LIMB IMAGING GEOMETRY  
TOP VIEW



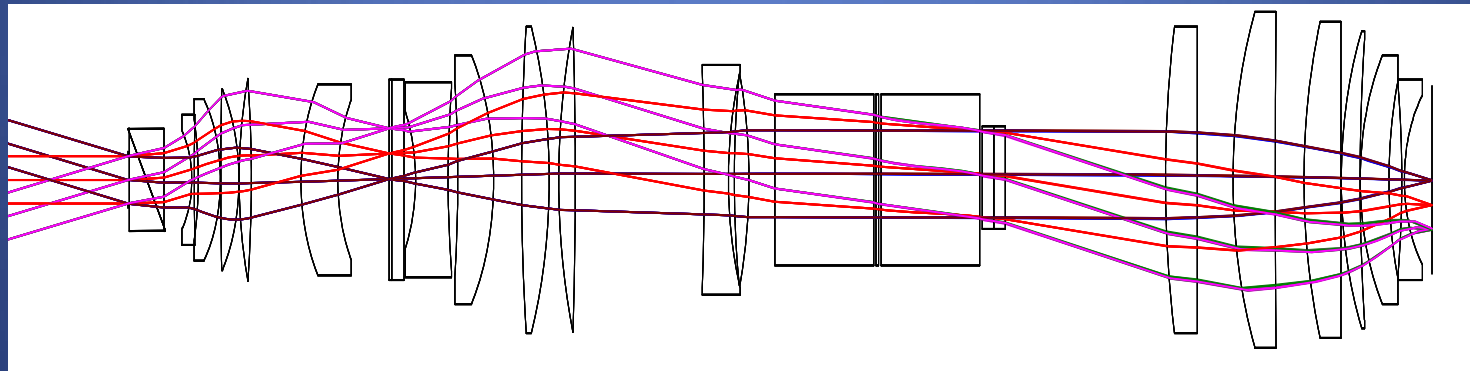
Parameter	Near-IR (Baseline)	Alternative or Supplemental Channel
Emission	O2 $^1\Delta$ @ 1.264 $\mu\text{m}$	OI $^1S$ @ 0.557 $\mu\text{m}$
Bandpass (filter)	$\sim 0.2$ nm	$\sim 1$ nm
Altitude Range	10 to 50 km	80 to 160 km
Field of View	$6^\circ \times 6^\circ$	$6^\circ \times 6^\circ$
View Directions	$45^\circ, 135^\circ, 225^\circ$ & $315^\circ$ wrt to S/C motion vector	
Aperture & F#	45 mm , f/2	45 mm , f/2
Detector	HgCdTe 1.6 $\mu\text{m}$ cutoff 40 $\mu\text{m}$ pixels 256x256	CCD (e2v 55-20) 22.5 $\mu\text{m}$ pixels 576x780
Vertical Bin	4 km	4 km
Integration Time	20 s	20 s
Path Difference	9 cm	7 cm (optimum)
Wind Sensitivity	$< 1$ to 4 m/s	1 to 10 m/s
Modes	Wind & Photometry (day) Photometry (night) (TBC)	Wind & Photometry (day) Photometry (night) (TBC)
Moving Parts	Filter Wheel (occasional) & Pointing Mirror (continuously stepped through views)	

Parameter	Requirement	Note
Mass	15.3 kg	
Envelope	60 x 34 x 23 cm	
Mounting	Kinematic to S/C	Alignment knowledge to S/C axes needed
Power	14 W (wind mode operating) 4 W (standby)	Peak power ~18W (during mechanism moves)
Cooling	Radiative (Detector at ~180K)	May be desirable to radiatively cool the instrument bench for stability
Radiator	Instrument mounted 120x120 mm	
Data Rate	2.5 Mbits/orbit	
Operations	Standby at night Observing day	
Pointing	Control : 0.2° Knowledge: 0.025° (yaw) Stability: 0.05°/min	
Orbit	350 km circular inclination TBD	Other altitudes and eccentricities are possible
Booms	None	
Deployments	None	
Mechanisms	Filter Wheel (periodic) Pointing Mirror (cont. cycle)	

# Polarization implementation



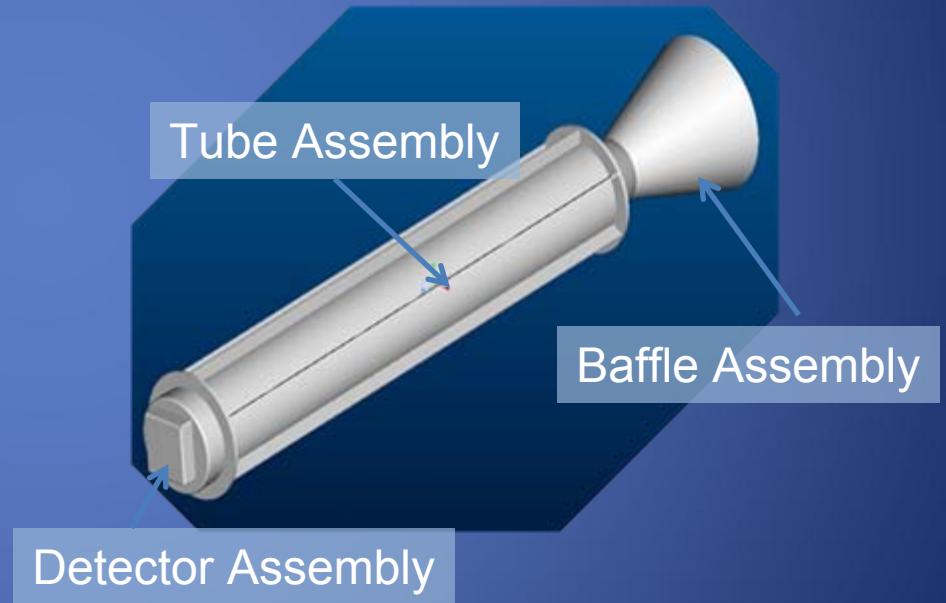
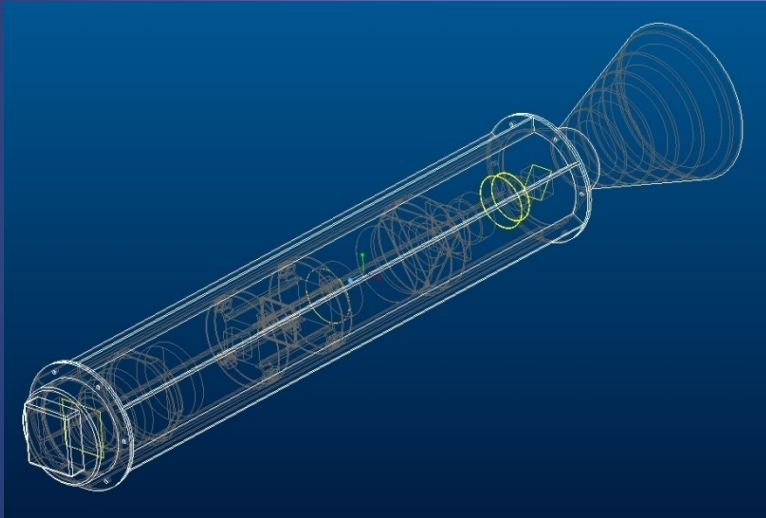
Schematic drawings of ANU birefringent interferometer (Howard, *et al.* 2000)



COM DEV optical layout,  $\frac{1}{4}$  field, of the optimized design. Performance prediction matches MIADI Michelson 9 degree field, with no moving components. All lenses are spherical and made of NBK7.

# Physical Accommodation

- Physical accommodation – low mass  $\sim 2\text{kg}$  optical head, no moving parts.



# SHS

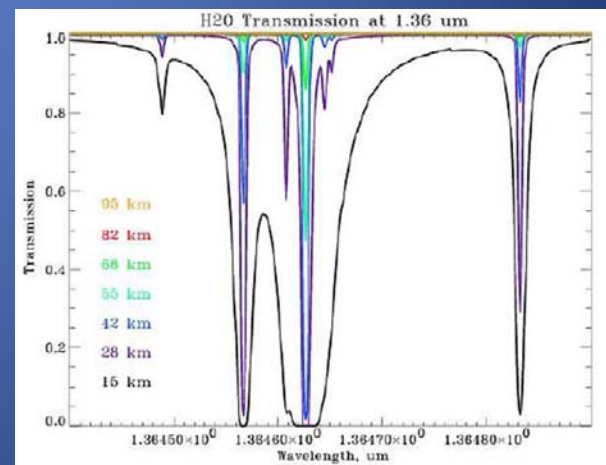
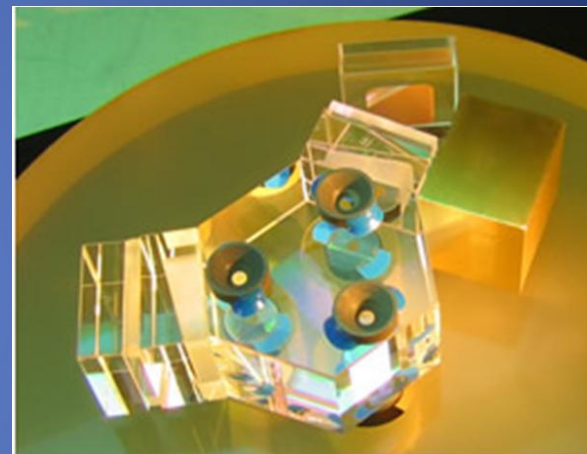
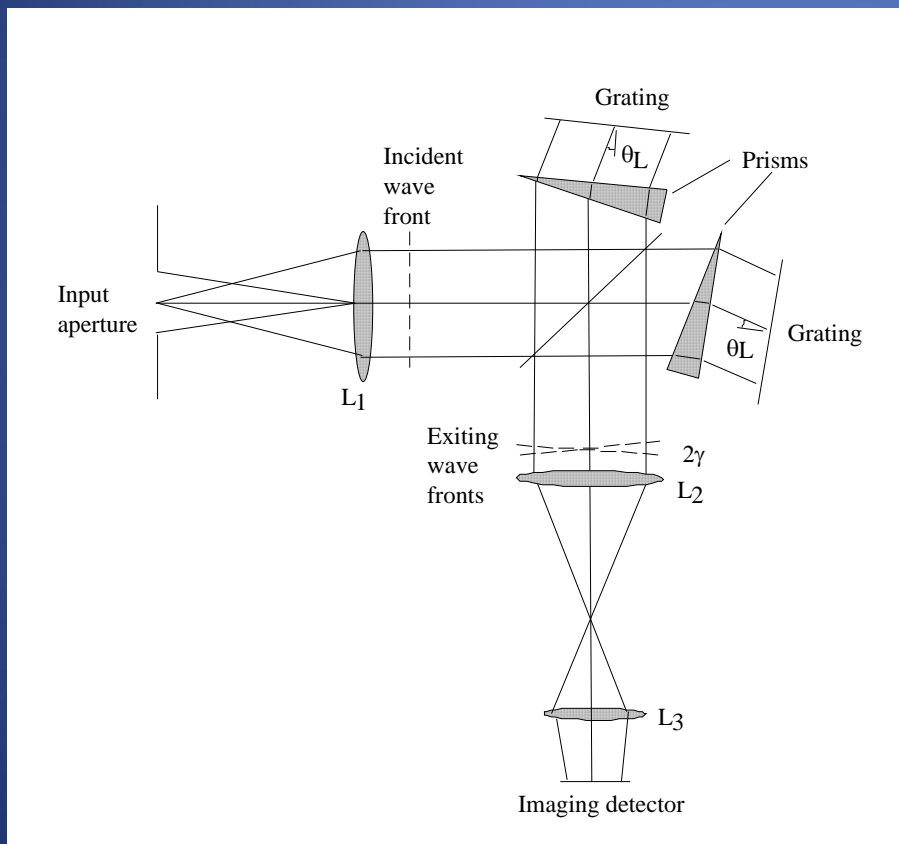
The spatial heterodyne spectrometer is a zero path difference Michelson in which tilted gratings in each arm replace the mirrors (above). Incident wavefronts experience opposite tilts based on the difference in wavelength from  $\lambda_L$ , the Littrow wavelength. This situation creates an interferogram on the detector in the direction perpendicular to the grating grooves.

This interferogram has zero spatial frequency at the Littrow wavelength, which is why it is called a spatial heterodyne. The other direction can be used to capture one dimension of spatial scene information. The basic (non field-widened) SHS superiority can be shown to be the same as other Michelson interferometers.

The spectral resolution of the SHS is set by the number of illuminated grating grooves, as in typical dispersive grating instruments, however there is no need for a slit in the instrument configuration, so the full aperture étendue is maintained throughout. Unlike FTS, the SHS spectral bandwidth needs to be limited by a narrow-band filter to prevent aliasing of nearby lines, limiting the effects of spectral multiplexing. Doppler measurements can be made by adding a phase delay to one of the arms.

The major advantage of SHS over FTS for space applications, is the lack of any moving parts, and the associated robustness this gives to the design. The spectral coverage of an SHS is limited by the number of pixels across the focal plane array (FPA) at the chosen resolution, rather than the motion of a mechanical apparatus.

# SHS diagrams



# Future Work

- A detailed analysis to optimize the emission selection and spatial/spectral imaging.
- Simulations of observation conditions for various orbits.
- Selection of the optimal interferometer configuration for the observations.